Multiple parton interactions and production of charged particles up to the intermediate-p_T range in high-multiplicity pp events at the LHC

Somnath Kar, Subikash Choudhury, Sanjib Muhuri, and Premomoy Ghosh*

Variable Energy Cyclotron Centre, HBNI, 1/AF Bidhan Nagar, Kolkata 700 064, India

(Received 19 October 2016; published 17 January 2017; publisher error corrected 23 January 2017)

Satisfactory description of data by hydrodynamics-motivated models, as has been reported recently by experimental collaborations at the LHC, confirm "collectivity" in high-multiplicity proton-proton (pp) collisions. Notwithstanding this, a detailed study of high-multiplicity pp data in other approaches or models is essential for better understanding of the specific phenomenon. In this study, the focus is on a pQCD-inspired multiparton interaction (MPI) model, including a color reconnection (CR) scheme as implemented in the Monte Carlo code, PYTHIA8 tune 4C. The MPI with the color reconnection reproduces the dependence of the mean transverse momentum $\langle p_T \rangle$ on the charged particle multiplicity $N_{\rm ch}$ in pp collisions at the LHC, providing an alternate explanation to the signature of "hydrodynamic collectivity" in pp data. It is, therefore, worth exploring how this model responds to other related features of high-multiplicity pp events. This comparative study with recent experimental results demonstrates the limitations of the model in explaining some of the prominent features of the final-state charged particles up to the intermediate-p_T ($p_T < 2.0$ GeV/c) range in high-multiplicity pp events.

DOI: 10.1103/PhysRevD.95.014016

I. INTRODUCTION

The long-range two-particle angular correlations in multiparticle production in high-multiplicity proton-proton (pp) events [1] at $\sqrt{s} = 7$ TeV at the Large Hadron Collider (LHC) resemble the results from similar studies in ultrarelativistic heavy-ion collisions, where the formation of a collective medium of partonic degrees of freedom is established [2–5]. The finding contradicts the prevailing knowledge of multiparticle production in hadronic collisions (pp or $p\overline{p}$) at pre-LHC (lower) energies and has resulted in enhanced activities in the study of the production mechanism of final-state particles in high-multiplicity pp events. Several theoretical and phenomenological studies in the search of a collective medium in high-multiplicity pp events have reported [6–13] a satisfactory description of the data. The idea of hydrodynamic collectivity in high-multiplicity pp events got strengthened with the pronounced signals revealed by the recent studies [14–16], including analysis of pp data at $\sqrt{s} = 13$ TeV at the LHC. More convincing signatures [17–21] of hydrodynamic flow in the proton-nucleus collisions, at the LHC and the Relativistic Heavy Ion Collider (RHIC), also support the applicability of hydrodynamic models in small systems. Still, before one surmises on the possibility of the formation of a collective medium in pp collisions, the unforeseen features need to be looked into through other conventional models.

The pQCD-inspired multiparton interaction (MPI) model along with the color reconnection (CR) scheme [22–24] has been proposed as an alternate explanation to the flow-like collective behavior of the final-state particles in high-multiplicity pp events. The model, implemented in the Monte Carlo code, PYTHIA8 tune 4C, successfully describes the dependence of the mean transverse momentum $\langle p_T \rangle$ on the charged particle multiplicity $N_{\rm ch}$ of pp collisions at $\sqrt{s} = 0.9$, 2.76 and 7 TeV, as measured [25] by ALICE in the kinematic ranges $|y| < 0.5$ and $p_T < 10$ GeV/c. According to the CR scheme, the multiparticle production in high-multiplicity events results from a large number of overlapped MPIs. The overlapped partons from individual MPIs get connected by color strings, and the partons cannot hadronize independently. The collective hadronization of reconnected partons from the overlapped MPIs takes place through a string fragmentation process. The effect of a transverse boost of the reconnected partons is manifested in the observed [25] flow-like dependence of $\langle p_T \rangle$ on $N_{\rm ch}$. It is worth noting here that the color reconnection explains the data including the high-p_T ($p_T < 10$ GeV/c) particles, while the signals of hydrodynamic collectivity are seen [7–12,15] up to the intermediate-p_T ($p_T < 2$ GeV/c) range. It is, therefore, important to study the responses of color reconnection up to the intermediate-p_T range only, for a better understanding of the relative effect of the collective hadronization due to color reconnection on the intermediate-p_T phenomena in high-multiplicity pp events. This article presents a comprehensive study on the comparison between the data and the MPI model, with and without color reconnection, in terms of several features of the multiparticle production up to the intermediate-p_T range in high-multiplicity pp events.

II. EVENT GENERATION

The conventional Monte Carlo event generators for pp collisions have different versions which include multiple

*prem@vecc.gov.in

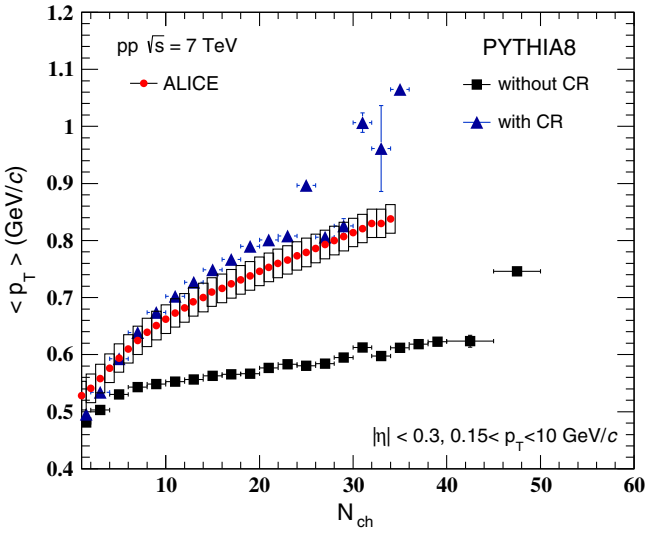

FIG. 1. The average transverse momentum, $\langle p_T \rangle$, as a function of charged particle multiplicity, $N_{\rm ch}$, as measured [25] by ALICE is compared with the simulated events of the PYTHIA8 tune 4C event generator with and without CR.

parton-parton interactions. Several of these versions are tuned to explain different features of the LHC pp data. In the context of the present study, the event generator PYTHIA8 tune 4C [22–24] is of interest. This particular version, by invoking the CR scheme, explains the ALICE measurement of the $N_{\rm ch}$ dependence of $\langle p_T \rangle$ in pp collisions up to $\sqrt{s} = 7$ TeV. In this study, we first reproduce the successful description of the ALICE result by PYTHIA. Using the tuned simulation code, we have generated 10^7 minimum-bias pp events at $\sqrt{s} = 7$ TeV, for each of the options, with and without CR. We have calculated $\langle p_T \rangle$ for charged particles of p_T up to 10 GeV/c, the same range used in the ALICE measurement. The reproduced plots are shown in Fig. 1. The simulated event sample from a tuned code that successfully reproduces a significant feature of particle production in pp collisions at the LHC energies can now be analyzed in terms of several observables for comparing with other features of the multiparticle production. We have analyzed the generated event samples in terms of transverse momentum (p_T) and two-particle angular correlations, with appropriate kinematic cuts and conditions to compare with several hydrodynamic-flow-related effects, as observed in the LHC experiments on pp collisions at $\sqrt{s} = 7$ TeV.

III. ANALYSIS AND RESULTS

A. Transverse momentum (p_T) / mass (m_T)

1. $\langle N_{\rm ch} \rangle$-dependent $\langle p_T \rangle$ for identified charged particles up to intermediate p_T

The reasonable success of the MPI model in explaining the $N_{\rm ch}$ dependence of $\langle p_T \rangle$ of unidentified charged particles up to the p_T range of 10 GeV/c encourages us to see how the MPI model with color reconnection fits into the nature of the multiplicity dependence of $\langle p_T \rangle$, obtained from the measured spectra of identified charged particles up to the intermediate-p_T range. We select subsamples from the generated event sample for studying the $N_{\rm ch}$ dependence of $\langle p_T \rangle$ for the identified charged particles in the same kinematic range as measured by the CMS experiment [26,27]. It is important to mention here that while ALICE has measured the $N_{\rm ch}$ dependence of $\langle p_T \rangle$, the CMS data, from which we obtain the $\langle p_T \rangle$ for the identified charged particles, are for different event classes, defined with $\langle N_{\rm tracks} \rangle$ [26]. Primarily, each of the event classes contains events with a range of the number of reconstructed charged particles. True-track multiplicity has been obtained by CMS from the reconstructed particles by comparing models from the simulation. The $\langle N_{\rm tracks} \rangle$ for each of the event classes has been obtained by taking the mean of the true-track multiplicities of events in the respective event class. In this article, we write $\langle N_{\rm tracks} \rangle$ as $\langle N_{\rm ch} \rangle$.

The CMS experiment has measured the p_T spectra of pions ($\pi^{\pm}$), kaons ($K^{\pm}$), and protons (p and $\overline{p}$) over the rapidity range $|y| < 1$ for the pp collisions at $\sqrt{s} = 0.9$, 2.76 and 7 TeV for several event classes in the pseudorapidity interval $|\eta| < 2.4$. The measured p_T ranges are 0.1 to 1.2 GeV/c for $\pi^{\pm}$, 0.2 to 1.050 GeV/c for $K^{\pm}$ and 0.35 to 1.7 GeV/c for p and $\overline{p}$. It is worth mentioning that the set of CMS spectra data used in this analysis meets the criterion of p_T range for analysis in terms of signals related to hydrodynamic collectivity. In fact, the same set of data, on analysis [12] in the hydrodynamics-motivated Boltzman-Gibbs blast-wave model [28], has revealed the collective transverse flow for the high-multiplicity pp events. For our analysis, we compute $\langle p_T \rangle$ of the measured identified charged particles for different event classes from pp collisions at $\sqrt{s} = 7$ TeV.

As is clear from Fig. 2, the CR causes an increase in the $\langle p_T \rangle$ of the charged particles in the simulated events for $N_{\rm ch} > 40$. Also, the increase in $\langle p_T \rangle$ has a $N_{\rm ch}$ dependence. However, the effect of the CR remains far from matching the measured $N_{\rm ch}$ dependence of $\langle p_T \rangle$ for the identified charged particles in the given kinematic ranges and multiplicities.

The wide mismatch between CMS data and the simulated events, in terms of the $N_{\rm ch}$ dependence of $\langle p_T \rangle$, prompts us to compare the identified charged particle spectra from the data and the simulated events.

2. Identified charged particle spectra

The p_T spectra of the produced particles contain information on temperature as well as the transverse expansion of a thermalized medium, if formed. The temperature-related information should ideally be reflected by the low-p_T particles (usually < 2 GeV/c, as has been considered in heavy-ion collisions).

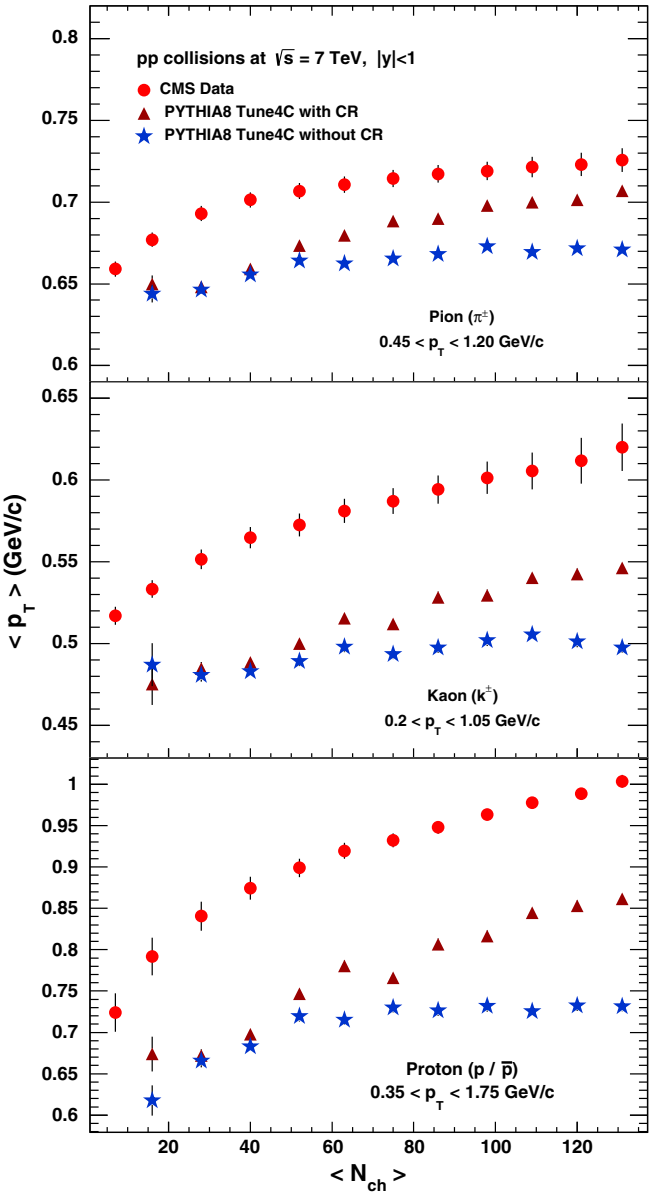

FIG. 2. Average transverse momentum, $\langle p_T \rangle$, for the identified charged particles in the pp collisions at $\sqrt{s} = 7$ TeV, as a function of mean charged particle multiplicity for several event classes. The CMS data [26,27] have been compared with simulated events using the PYTHIA8 tune 4C event generator with and without CR.

The slope of the transverse mass (m_T) spectra for identified charged particles that can be obtained from the p_T spectra [for a particle of mass m, $m_T = (m^2 + p_T^2)^{1/2}$], is used for comparing thermal states of the system. The m_T spectra corresponding to low-p_T particles are usually satisfactorily fitted with an exponential function of the form

$$\frac{dN}{m_T dm_T} = C \times \exp\left(-\frac{m_T}{T_{\text{effective}}}\right), \tag{1}$$

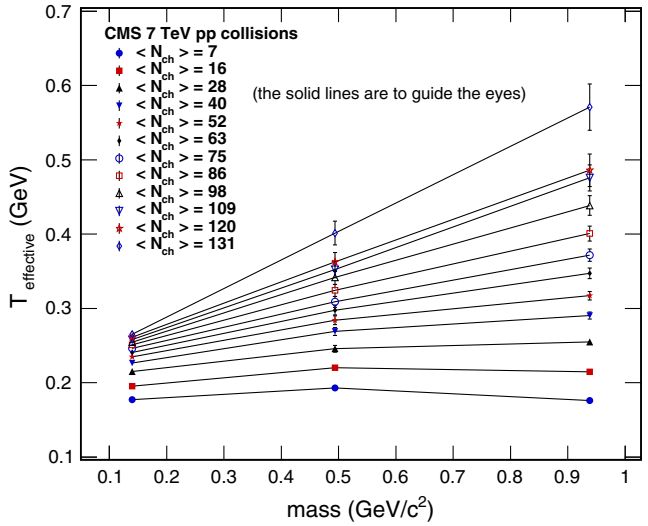

FIG. 3. The inverse slope parameter $T_{\text{effective}}$ as a function of the masses of identified charged particles ($m_{\pi^\pm} = 0.14$, $m_{K^\pm} = 0.495$, $m_{p(\bar{p})} = 0.938$ GeV/c^2) produced in pp collisions [26,27] at $\sqrt{s} = 7$ TeV. $\langle N_{\text{ch}} \rangle$ is the mean multiplicity of the charged particles representing event classes.

where $T_{\text{effective}}$, known as the inverse slope parameter, contains information about the temperature as well as the effect due to transverse expansion of the system.

The increase in the inverse slope parameter $T_{\text{effective}}$ with mass m for the most commonly measured and identified charged particles ($\pi^\pm$, $K^\pm$, p and $\overline{p}$), that has been observed in heavy-ion [29,30] and recent proton-lead collisions [31] at the LHC, is a well-known phenomenon, attributed to the collective flow of the medium formed in the collision. We look for the mass dependence of the inverse slope parameter by fitting the m_T spectra data of identified charged particles obtained from the overlapped range ($0.475 < p_T < 1.025$) of the p_T spectra at $\sqrt{s} = 7$ TeV, as measured [27] by the CMS experiment. The increase of $T_{\text{effective}}$ with the mass of identified charged particles for event classes of high $\langle N_{\text{ch}} \rangle$, as has been depicted in Fig. 3, reiterates the finding of a collective medium in high-multiplicity pp events. The mass ordering of the inverse slope parameter becomes steeper with the event classes of higher $\langle N_{\text{ch}} \rangle$. Comparing the mass ordering for different multiplicity classes, we note that the data show a relatively large increase in the inverse slope parameters from the multiplicity class of $\langle N_{\text{ch}} \rangle = 120$ to $\langle N_{\text{ch}} \rangle = 131$.

To compare the measured spectra with those from the simulated pp events, we initially chose the event class of the highest multiplicity, identified by $\langle N_{\text{ch}} \rangle = 131$. In Fig. 4, the identified charged particle spectra as a function of the transverse mass for $\pi^\pm$, $K^\pm$ and p & $\overline{p}$, obtained from the measured p_T spectra [26,27] and from the simulation with and without CR, for $0.475 < p_T < 1.025$ and for the multiplicity class of $\langle N_{\text{ch}} \rangle = 131$, are plotted.

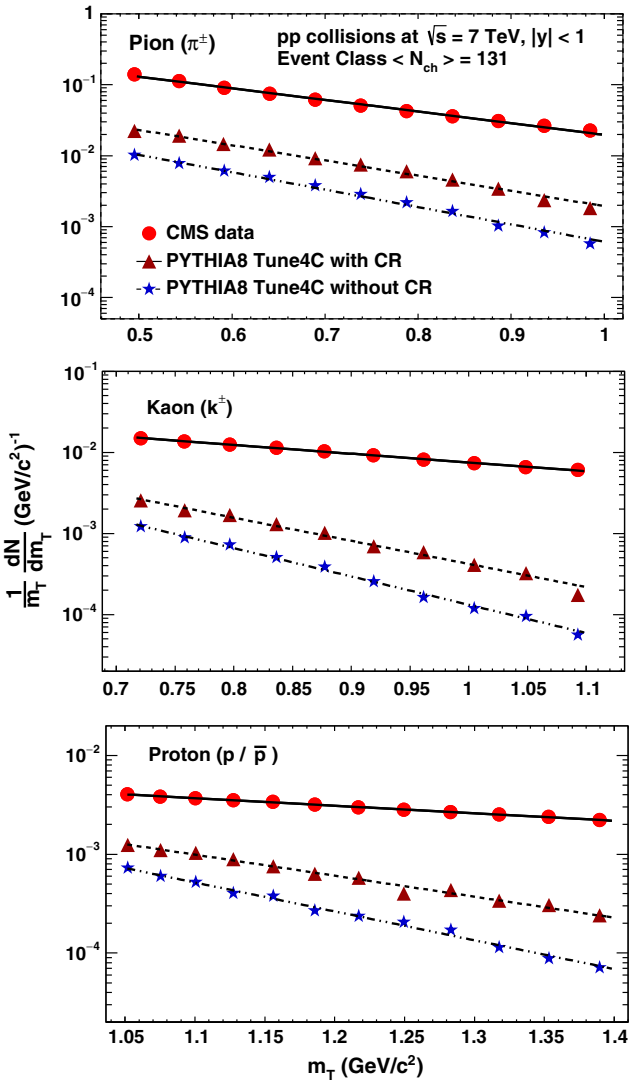

FIG. 4. m_T spectra for identified charged particles as obtained from the CMS data [26,27] of pp collisions at $\sqrt{s} = 7$ TeV. The data are compared with the simulated events using the PYTHIA8 tune 4C event generator with and without CR.

We fit the spectra with the exponential function not for the temperature estimation, but just for a quantitative comparison of the spectra from the experiment and the simulation in terms of the inverse slope parameter. The values of the best fits to the spectra, as obtained in terms of χ^2/NDF, using the MINUTE program in the ROOT analysis framework [32], are listed in Table I. Keeping in mind the relatively large increase in the inverse slope parameters from the multiplicity class of $\langle N_{\rm ch}\rangle = 120$ to $\langle N_{\rm ch}\rangle = 131$ (Fig. 3), for a consistency check, we repeat the comparison of the measured identified charged particle spectra with those from the PYTHIA-generated events for the multiplicity class of $\langle N_{\rm ch}\rangle = 120$ also. The best fitted values of the parameter and corresponding χ^2/NDF for the event class $\langle N_{\rm ch}\rangle = 120$ are added to Table I. From the values tabulated in Table I, it is clear that while the high-multiplicity pp data exhibit mass ordering of the inverse slope parameter of the m_T distributions, the simulated PYTHIA events—with or without CR—do not exhibit such mass ordering. The largely deviated inverse slope parameters for the simulated events from the ones obtained from the measured spectra establish the disagreement between the data and the simulated events.

B. Two-particle angular correlations

1. The correlation function

The observed limitation of the MPI with color reconnection in explaining the $N_{\rm ch}$ dependence of $\langle p_T\rangle$ for the identified charged particles with $p_T < 2.0$ GeV/c leads us to think that the model may not really provide an alternate explanation to the features, considered to be due to the hydrodynamic collectivity. We therefore proceed to check the responses of the model to the analysis in terms of the two-particle angular correlations giving rise to "long-range near-side associated yields," a measure of correlations that is attributed to the formation of a collective medium. In the very recent analysis of pp data including those from collisions at $\sqrt{s} = 13$ TeV at the LHC, also, the two-particle angular correlations study has "confirmed" [14–16] the formation of a collective medium in high-multiplicity pp events by extracting [14,16] the anisotropy coefficient, v_2. While the mass ordering of $v_2(p_T)$ for the identified charged particles has been observed [16], the p_T dependence of v_2, similar to that observed in the proton-lead and the lead-lead collisions, has also been revealed [14]. It may be worth mentioning at this point that these v_2-related features have been explained [33] in an alternate approach in the IP-Glasma model, based on color glass condensate, followed by the Lund string fragmentation algorithm of PYTHIA. In Ref. [33], it has been shown that further tuning of the p_T-smearing fragmentation parameter in the default PYTHIA can have a significant effect on the two-particle correlation function, and reproduce the experimental results on the p_T dependence of v_2 for pp collisions. In this paper, however, we continue to contrast the MPI model, as implemented in the default PYTHIA, with the pp data [15] at $\sqrt{s} = 7$ TeV only, as the same PYTHIA version reproduces (Fig. 1) the ALICE results of the $N_{\rm ch}$ dependence of $\langle p_T\rangle$ for pp collisions at $\sqrt{s} = 7$ TeV. It may be mentioned that the multiplicity-dependent analysis [15] of pp data at $\sqrt{s} = 7$ and 13 TeV by the CMS Collaboration has established that, for a given multiplicity, there has been no energy dependence of the "long-range near-side associated yields."

The two-particle angular correlation function, used in this analysis, is characterized by the $\Delta\eta$, $\Delta\varphi$ distribution (where $\Delta\eta$ and $\Delta\varphi$ are differences in the pseudorapidity (η) and the azimuthal angle (φ) of the two particles) of the per-trigger particle yield of associated charged particles and is given by [15]

TABLE I. The inverse slope parameters of the exponential fits to the m_T spectra of $\pi^{\pm}$, $K^{\pm}$ and p & $\bar{p}$ for the multiplicity classes $\langle N_{\rm ch}\rangle = 131$ and 120 for pp collisions at $\sqrt{s} = 7$ TeV, obtained from the CMS data [26,27] and the simulated events using the PYTHIA8 tune 4C event generator with and without color reconnection.

Identified particles	Data		MPI with CR		MPI without CR	
	$T_{\rm eff}$	$\frac{\chi^2}{NDF}$	$T_{\rm eff}$	$\frac{\chi^2}{NDF}$	$T_{\rm eff}$	$\frac{\chi^2}{NDF}$
			$\langle N_{\rm ch}\rangle = 131$			
$\pi^{\pm}$	0.265 ±0.002	5.432	0.202 ±0.001	28.224	0.177 ±0.001	28.18
$K^{\pm}$	0.401 ±0.016	0.084	0.152 ±0.002	6.612	0.124 ±0.001	3.313
$(p, \bar{p})$	0.571 ±0.031	0.039	0.204 ±0.004	2.596	0.148 ±0.002	2.326
			$\langle N_{\rm ch}\rangle = 120$			
$\pi^{\pm}$	0.261 ±0.003	5.578	0.196 ±0.001	27.701	0.174 ±0.001	9.364
$K^{\pm}$	0.362 ±0.013	0.082	0.151 ±0.002	5.682	0.128 ±0.002	5.967
$(p, \bar{p})$	0.486 ±0.022	0.008	0.197 ±0.005	2.059	0.151 ±0.003	4.429

$$\frac{1}{N_{\rm trig}}\frac{d^2N^{\rm assoc}}{d\Delta\eta d\Delta\varphi} = B(0,0)\times\frac{S(\Delta\eta,\Delta\varphi)}{B(\Delta\eta,\Delta\varphi)}, \quad (2)$$

where $N_{\rm trig}$ is the number of trigger particles.

The function $S(\Delta\eta,\Delta\varphi)$ is the differential measure of the per-trigger distribution of associated hadrons in the same event, i.e.

$$S(\Delta\eta,\Delta\varphi) = \frac{1}{N_{\rm trig}}\frac{d^2N^{\rm assoc}_{\rm same}}{d\Delta\eta d\Delta\varphi}. \quad (3)$$

The same-event distribution functions are corrected for the random combinatorial background and effects due to the limited acceptance. This is usually done by dividing the same-event distribution function by the mixed-event background distribution, where the trigger and associated particles are paired from two different events of similar multiplicity.

The background distribution function $B(\Delta\eta,\Delta\varphi)$ is defined as

$$B(\Delta\eta,\Delta\varphi) = \frac{d^2N^{\rm mixed}}{d\Delta\eta d\Delta\varphi}, \quad (4)$$

where $N^{\rm mixed}$ is the number of mixed-event pairs.

The factor $B(0,0)$ in Eq. (2) is used to normalize the mixed-event correlation function such that it is unity at $(\Delta\eta,\Delta\varphi) = (0,0)$. Finally, the acceptance corrected correlation function is determined by scaling the same event distribution function, $S(\Delta\eta,\Delta\varphi)$, by the inverse of the normalized background distribution function, $B(\Delta\eta,\Delta\varphi)/B(0,0)$.

The "short-range" ($|\Delta\eta| \sim 0$) two-particle azimuthal angle correlations are dominated by jets, produced in the hard QCD scattering. As the jets are produced back to back in azimuth, the jet correlations are reflected in the $|\Delta\varphi|$ distribution. The jet-induced per-trigger hadron-pair yields from the same jet populate at $|\Delta\varphi| = (|\varphi_{\rm trigger} - \varphi_{\rm assoc}|) \sim 0$. The pair yields from the away-side jets show up at $|\Delta\varphi| = (|\varphi_{\rm trigger} - \varphi_{\rm assoc}|) \sim \pi$.

In relativistic heavy-ion collisions, the "long-range" ($|\Delta\eta| \gg 0$) two-particle azimuthal angle correlations have been attributed to the formation of a collective partonic medium. The per-trigger pair yields, with small $|\Delta\varphi|$ over a wide range of $|\Delta\eta|$ (long range), result in a "ridge" structure in the constructed correlation functions. The ridge structure also appears in the high-multiplicity pPb [17–19] and pp [1,14–16] events at the LHC. The analysis [15] of the LHC pp data in terms of the correlated yields as a function of $|\Delta\varphi|$ reveals that the long-range ridge structure at $|\Delta\varphi| \sim 0$ increases with the multiplicity of pp events. It is these near-side long-range correlations, or the "ridge-like" correlations, that are of particular interest for the present study and for the general understanding of multiparticle production in high-multiplicity pp events. In this analysis, in terms of the two-particle angular correlations, we focus on the ridge-like correlations only and choose to contrast the MPI model with the published results [15,34].

2. Extraction of long-range near-side associated yield

For an optimum comparison with the experimental results on multiplicity-dependent correlation analysis, in terms of the near-side associated yield in the long range, the generated minimum bias events, with and without the CR scheme, at $\sqrt{s} = 7$ TeV have been divided into different multiplicity classes following the criteria adopted in Ref. [15]. The two-particle correlation functions have been

TABLE II. Multiplicity classes and the corresponding number of simulated events used for correlation analysis. The multiplicity ranges have been chosen following similar classification to that adopted in Ref. [15].

Multiplicity bin	Number of events (in millions)	
	with *CR*	without *CR*
$2 \leq N_{\rm ch} < 35$	6.1	5.4
$35 \leq N_{\rm ch} < 90$	2.3	2.2
$90 \leq N_{\rm ch} < 110$	0.2	0.4
$N_{\rm ch} \geq 110$	0.8	0.6

constructed for each of the multiplicity classes of simulated events to compare with the data [15] of similar multiplicity classes and in the same ranges of transverse momentum (p_T) and pseudorapidity (η). It is important to note here that the latest p_T-dependent study [15] reveals that the near-side long-range correlations are strongest in the range $1.0 < p_T < 2.0$ GeV/c. We construct the two-dimensional correlation function in $(\Delta\eta, \Delta\varphi)$ in the same p_T range. For the long-range correlations, the two-dimensional correlation functions are projected onto the $\Delta\varphi$ axis for $2.0 < |\Delta\eta| < 4.0$. The multiplicity classes and the total number of events analyzed in each class are given in Table II.

Figure 5 shows the multiplicity-dependent one-dimensional $\Delta\varphi$ distribution as extracted by the CMS experiment in pp collisions at $\sqrt{s} = 7$ TeV, together with the results of the PYTHIA events of similar multiplicity and identical range of particle transverse momentum for the $\Delta\eta$ range, $2.0 < |\Delta\eta| < 4.0$. The one-dimensional $\Delta\varphi$ distribution is extracted from the two-dimensional correlation function. It is clear from the Fig. 5, for both of the simulated event classes (with and without CR), that the $\Delta\varphi$ distributions in the range of small $\Delta\varphi$ are close to zero for low-multiplicity events, in agreement with the data. The distributions obtained from the high-multiplicity simulated events, including those generated by invoking the CR, continue to coincide with zero, contradicting the data [15,34].

The comparison of the multiplicity dependence of long-range near-side correlations between the data and the simulated events is better represented in terms of the long-range near-side associated yields. To reduce the statistical fluctuations in baseline estimation, conventionally, the one-dimensional correlation distribution over the entire 2π range is reflected/folded into $0 < \Delta\varphi < \pi$. The baseline for calculating the correlated associated yield is considered here as a straight-line parallel to the $\Delta\varphi$ axis that passes through the point of minimum yield. The long-range associated yield above the baseline is calculated by the bin-counting method. The near-side long-range associated yields as calculated from the PYTHIA-generated events are plotted in Fig. 6 along with the results from data, obtained from Refs. [15,34].

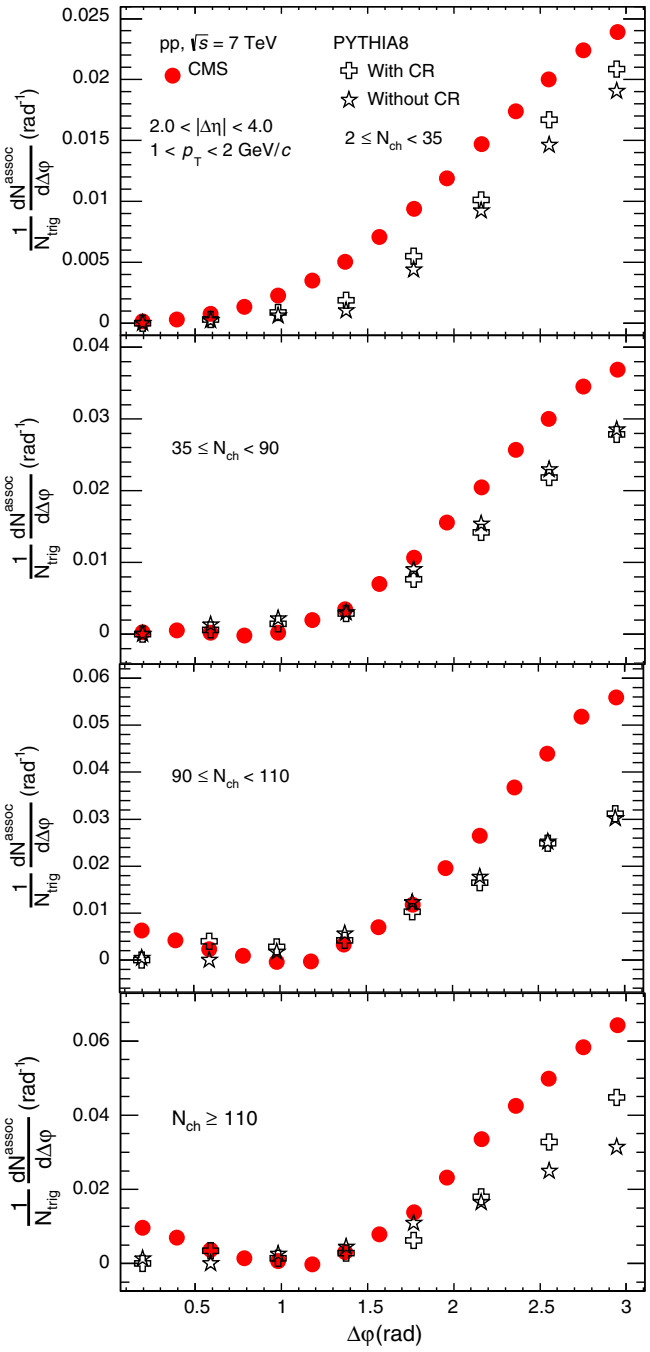

FIG. 5. One-dimensional $\Delta\varphi$ projection for the region of ridge-like correlations from the data [15,34] and for the simulated events by PYTHIA.

It is worth discussing at this point that the calculation of yield above the baseline is very sensitive to the statistics. So, instead of quantitative comparison between the yields from data and the simulation, we prefer to compare the relative trend of multiplicity-dependent yields. As has been depicted in Fig. 6, while the yields for the simulated event samples have no multiplicity dependence, the data exhibit clear nonzero values for the high-multiplicity

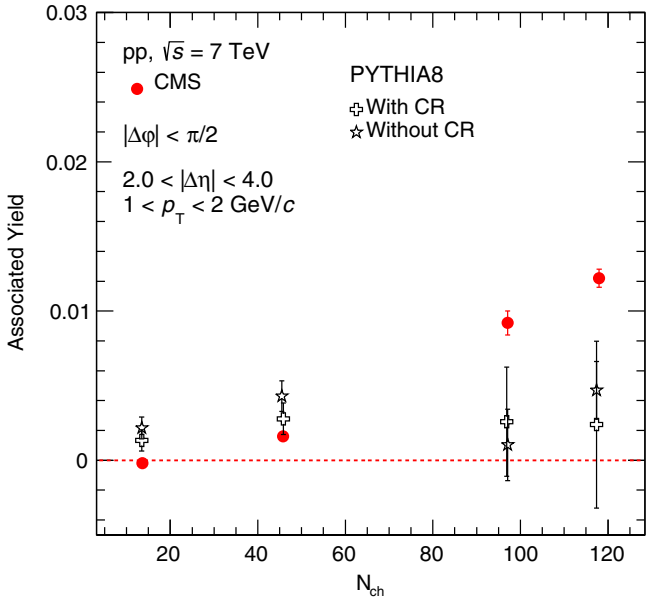

FIG. 6. Comparison of multiplicity-dependent near-side ridge-like associated yields for the data [15,34] and simulated PYTHIA events.

event classes with an increasing trend of multiplicity dependence.

The results from our analysis in terms of two-particle angular correlations clearly indicate that the MPI model with or without the CR scheme cannot explain the long-range ridge-like correlations observed in high-multiplicity pp events.

We would like to mention that an exercise to match the data by tuning the related color reconnection parameter in the simulation code PYTHIA8 tune 4C would be interesting. In this study, however, we do not attempt to tune any parameter of the event generator version that successfully describes the data including particles in the high-p_T ($p_T < 10$ GeV/c) range, as our objective has been to see the response of the same version of the event generator to the phenomena, relevant up to the intermediate-p_T ($p_T < 2$ GeV/c) range only.

IV. SUMMARY AND CONCLUSION

We have studied the PYTHIA-generated events in the multiple-parton interaction model with and without color reconnection. Our analysis was aimed at contrasting the MPI model with the multiparticle production data of high-multiplicity pp events in the intermediate-p_T range, that carries information of the collective medium, if any, formed in the collisions.

In terms of the p_T distributions and related observables, the analysis reveals that the $N_{\rm ch}$ dependence of $\langle p_T \rangle$ for identified charged particles up to the intermediate-p_T range in simulated events does not match the data. Though the CR scheme gives a boost to the $\langle p_T \rangle$ of the identified particles for $N_{\rm ch} > 40$, it is not enough to describe the data. In the lower range of $N_{\rm ch}$, the CR has no effect on $\langle p_T \rangle$.

The CR in the MPI model also cannot describe the identified charged particle spectra from the high-multiplicity pp events up to the intermediate p_T. Further, while the data exhibit the mass ordering of the inverse slope parameter of the identified charged particle spectra for the high-multiplicity pp events, the simulated events—with and without CR—do not show any such ordering.

The MPI model, by invoking the CR scheme also, cannot describe the ridge-like structure in the two-particle angular correlations in the high-multiplicity pp data.

The color reconnection in the MPI model, by successful description of the multiplicity ($N_{\rm ch}$) dependence of the mean transverse momentum ($\langle p_T \rangle$) of produced particles up to $p_T < 10$ GeV/c, indicates the collective hadronization in pp collisions at the LHC energies. This study reveals that the color reconnection does not provide a full explanation of the collective feature in pp collisions. In the high-multiplicity pp events, the model cannot account for the flow-like effects in the intermediate-p_T ($p_T < 2$ GeV/c) range, where the hydrodynamic models appear to be convincing. In the description of high-multiplicity pp events at the LHC, therefore, while the collective effect in the intermediate-p_T domain can be modeled with hydrodynamic flow, the contribution of color reconnection may be taken into consideration in the hadronization phase.

ACKNOWLEDGMENTS

The authors are thankful to the members of the grid computing team of VECC for providing uninterrupted facility for event generation.

[1] V. Khachatryan *et al.* (CMS Collaboration), J. High Energy Phys. 09 (2010) 091.
[2] I. Arsene *et al.* (BRAHMS Collaboration), Nucl. Phys. **A757**, 1 (2005).
[3] B. B. Back *et al.* (PHOBOS Collaboration), Nucl. Phys. **A757**, 28 (2005).
[4] J. Adams *et al.* (STAR Collaboration), Nucl. Phys. **A757**, 102 (2005).

[5] K. Adcox *et al.* (PHENIX Collaboration), Nucl. Phys. **A757**, 184 (2005).
[6] P. Bozek, Eur. Phys. J. C **71**, 1530 (2011).
[7] K. Werner, I. Karpenko, and T. Pierog, Phys. Rev. Lett. **106**, 122004 (2011).
[8] R. Campanini and G. Ferri, Phys. Lett. B **703**, 237 (2011).
[9] M. Csnad and T. Csorgo, Proc. EDS Blois **2013**, 53 (2013).
[10] A. Kisiel, Phys. Rev. C **84**, 044913 (2011).
[11] E. Shuryak and I. Zahed, Phys. Rev. C **88**, 044915 (2013).
[12] P. Ghosh, S. Muhuri, J. Nayak, and R. Varma, J. Phys. G **41**, 035106 (2014).
[13] I. Bautista, A. F. Tellez, and P. Ghosh, Phys. Rev. D **92**, 071504(R) (2015).
[14] G. Aad *et al.* (ATLAS Collaboration), Phys. Rev. Lett. **116**, 172301 (2016).
[15] V. Khachatryan *et al.* (CMS Collaboration), Phys. Rev. Lett. **116**, 172302 (2016).
[16] V. Khachatryan *et al.* (CMS Collaboration), Phys. Lett. B **765**, 193 (2017).
[17] B. Ablev *et al.* (ALICE Collaboration), Phys. Lett. B **719**, 29 (2013).
[18] S. Chatrchyan *et al.* (CMS Collaboration), Phys. Lett. B **718**, 795 (2013).
[19] G. Aad *et al.* (ATLAS Collaboration), Phys. Rev. Lett. **110**, 182302 (2013).
[20] B. Ablev *et al.* (ALICE Collaboration), Phys. Lett. B **728**, 25 (2014).
[21] A. Adare *et al.* (PHENIX Collaboration), Phys. Rev. Lett. **114**, 192301 (2015).
[22] A. O. Velasquez, P. Christiansen, E. C. Flores, I. A. M. Cervantes, and G. Paic, Phys. Rev. Lett. **111**, 042001 (2013).
[23] T. Sjostrand and M. van Zijl, Phys. Rev. D **36**, 2019 (1987).
[24] I. A. Maldonado-Cervantes, E. Cuautle, G. Paic, A. O. Velasquez, and P. Christiansen, J. Phys. Conf. Ser. **509**, 012064 (2014).
[25] B. Abelev *et al.* (ALICE Collaboration), Phys. Lett. B **727**, 371 (2013).
[26] V. Khachatryan *et al.* (CMS Collaboration), Eur. Phys. J. C **72**, 2164 (2012).
[27] The Durham HepData Project Collaboration, http://hepdata.cedar.ac.uk/view/ins1123117.
[28] E. Schnedermann, J. Sollfrank, and U. Heinz, Phys. Rev. C **48**, 2462 (1993).
[29] I. G. Bearden *et al.* (NA44 Collaboration), Phys. Rev. Lett. **78**, 2080 (1997).
[30] N. Xu, Prog. Part. Nucl. Phys. **53**, 165 (2004).
[31] S. Chatrchyan *et al.* (CMS Collaboration) Eur. Phys. J. C **74**, 2847 (2014).
[32] CERN/ROOT/v123.
[33] B. Schenke, S. Schlichting, P. Tribedy, and R. Venugopal, Phys. Rev. Lett. **117**, 162301 (2016).
[34] The Durham HepData Project Collaboration, http://hepdata.cedar.ac.uk/view/ins1397173.